



HHS Public Access

Author manuscript

Colloids Surf B Biointerfaces. Author manuscript; available in PMC 2017 November 01.

Published in final edited form as:

Colloids Surf B Biointerfaces. 2016 November 1; 147: 492–500. doi:10.1016/j.colsurfb.2016.07.048.

Multifunctional Organically Modified Silica Nanoparticles for Chemotherapy, Adjuvant Hyperthermia and Near Infrared Imaging

Abhignyan Nagesetti^a and Anthony J McGorona^a

^aBiomedical Engineering Department, Florida International University, 10555 West Flagler Street, EC 2614, Miami, FL 33174, USA

Abstract

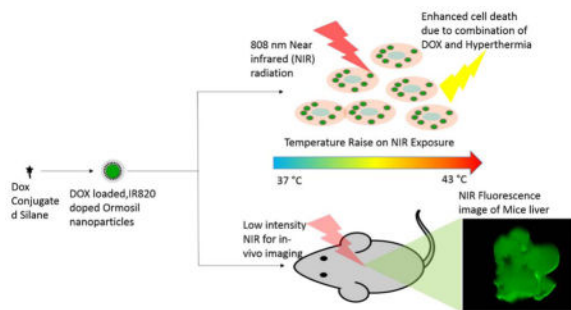
We report a novel system of organically modified silica nanoparticles (Ormosil) capable of near infrared fluorescence and chemotherapy with adjuvant hyperthermia for image guided cancer therapy. Ormosil np's were loaded with a chemotherapeutic, Doxorubicin (DOX) and cyanine dye, IR820. Ormosil particles had a mean diameter of 51.2 ± 2.4 nanometers and surface charge of -40.5 ± 0.8 millivolts. DOX was loaded onto Ormosil particles via physical adsorption (FDSIR820) or covalent linkage (CDSIR820) to the silanol groups on Ormosil surface. Both formulations retained DOX and IR820 over period of 2 days in aqueous buffer, though CDSIR820 retained more DOX (93.2%) compared to FDSIR820 (77.0 %) nanoparticles. Exposure to near infrared laser triggered DOX release from CDSIR820. Uptake of nanoparticles was determined by deconvolution microscopy in ovarian carcinoma cells (Skov-3). CDSIR820 localized in the cell lysosomes whereas, cells incubated with FDSIR820 showed DOX fluorescence from the nucleus indicating leakage of DOX from the nanoparticle matrix. FDSIR820 nanoparticles showed severe toxicity in Skov-3 cells whereas, CDSIR820 particles had the same cytotoxicity profile as Bare (No DOX and IR820) Ormosil particles. Furthermore, exposure of CDSIR820 nanoparticles to Near Infrared laser at 808 nanometers resulted in generation of heat (to 43°C from 37°C) and resulted in enhanced cell killing compared to Free DOX treatment. Bio-distribution studies showed that CDSIR820 nanoparticles were primarily present in the organs of Reticuloendothelial (RES) system.

Graphical Abstract

A novel multifunctional theranostic probe based on ormosil silica nanoparticles for in-vivo imaging and combination of chemotherapy with adjuvant hyperthermia (43°C).

mcgorona@fiu.edu; Fax: +1-305-348-6954; Tel: +1-305-348-1352.

Publisher's Disclaimer: This is a PDF file of an unedited manuscript that has been accepted for publication. As a service to our customers we are providing this early version of the manuscript. The manuscript will undergo copyediting, typesetting, and review of the resulting proof before it is published in its final citable form. Please note that during the production process errors may be discovered which could affect the content, and all legal disclaimers that apply to the journal pertain.



1. Introduction

Adjuvant therapies, such as the combination of chemotherapy and heat (hyperthermia; 43°C– 45°C) have been shown to have super additive or synergistic effect on cancer cell killing. Our group has shown that the combination of Doxorubicin (DOX) chemotherapy and hyperthermia induced by laser exposure of Near Infrared (NIR) Dyes such as Indocyanine Green (ICG) resulted in enhanced cancer cell killing compared to individual treatments.¹ NIR dyes also provide the advantage of imaging at infrared wavelengths where the absorption and scattering by surrounding tissues not having the NIR agent is minimal. Therefore, the combination of NIR dyes and DOX is ideal for image guided chemotherapy and adjuvant hyperthermia. An alternative to ICG (FDA approved for in-vivo applications) is IR820 which is more stable than ICG in aqueous solutions and has twice the degradation half-life (24.75 hours) of ICG.² However, in-vivo administration of IR820 in its free form results in rapid elimination (elimination half-life: 30.76 hours)² and lacks specificity to target tumor regions. Similarly, DOX also lacks specificity to tumor cells and is toxic to healthy cells, which leads to long term side effects, most notably severe cardiotoxicity. Hence, the success of chemotherapy and adjuvant NIR hyperthermia in-vivo is dependent on the stability and simultaneous availability of both agents at the tumor site. This is achieved through nanoparticles.

Nanoparticles are ideal carriers for simultaneous delivery of therapeutic and diagnostic probes (theranostic) to the tumor site. They can shield healthy tissues from toxic drug exposure and owing to their size are capable of passive targeting of tumor tissues via the enhanced permeation and retention (EPR) effect. We have recently shown the formulation of Poly-Lactic-co-Glycolic acid nanoparticles encapsulated with DOX and ICG (DOX-ICG-PLGA)³ and nanoparticles with a novel temperature sensitive polymer, Poly (Glycerol Malate co-Dodecanedioate) (PGMD) encapsulated with DOX and IR820 (DOX-IR820-PGMD).⁴ Both nanoparticles were able to successfully circumvent the P-gp mediated drug resistance in uterine sarcoma cells (Mes-sa/Dx5) and exposure to NIR hyperthermia enhanced the cell killing (compared to DOX alone) in DOX insensitive ovarian carcinoma cells (Skov-3).⁵ Additionally, DOX-ICG-PGMD particles showed enhanced DOX release in response to lower pH (pH = 5.0) and also to heat generated by laser exposure of IR820 dye.⁴ However, the nanoparticles suffered limitations due to inherent properties of the polymers. DOX-ICG-PLGA and DOX-ICG-PGMD particles had high initial release (burst) of DOX immediately on resuspension in aqueous media and a non-optimal size (> 100 nm) for cell

uptake and tumor penetration. Also, the imaging and hyperthermia agent, IR820 was released from the particle upon injection in-vivo. This is disadvantageous for tumor specific imaging (low signal to noise ratio) and reduces the thermal dose delivered at the tumor. The goal of image guided chemotherapy, as we propose, is for the imaging and hyperthermia agent to be retained in the nanoparticle and chemotherapeutic to be released in response to the microenvironment of tumors (low pH) or to an external stimulus (heat or laser exposure). This will ensure highly specific chemotherapy and adjuvant hyperthermia at the tumor site while mitigating DOX associated side effects.

We report the creation of organically modified silica nanoparticles (Ormosil Np's) loaded with DOX and IR820 with optimal size (~50 nm) with slow release properties of DOX and IR820 suitable for long term cancer imaging and adjuvant hyperthermia. In this system DOX serves as the chemotherapeutic and IR820 is for NIR in-vivo imaging and adjuvant hyperthermia. Ormosil Np's were pioneered by Prasad *et al.* using a ternary microemulsion system comprised of an oil phase, surfactant, co-surfactant and aqueous phase.⁶ The precursor molecule is an organic silane monomer viz Triethoxyvinylsilane (VTES). The parameters of the microemulsion can be varied to achieve particles in size ranging from 25 nm to 80 nm. Ormosil Np's have been used for chemotherapeutic, photodynamic, gene delivery and bio imaging applications.⁷⁻⁹ Multifunctional Ormosil Np's entrapped with iron oxide particles and a fluorophore have been reported for MRI and optical imaging applications.^{10,11} However, multifunctional Ormosil Np's for image guided cancer therapy have not been developed until now.

The NIR dye IR820 was entrapped inside the silica matrix whereas DOX was loaded via physical adsorption (called FDSIR820) or via a covalent linkage (called CDSIR820) on the surface of the Ormosil Np's. A silica shell was grown over the DOX layer and was functionalized with amine (-NH₂) groups. Functionalization with amine groups offers the flexibility of further modifying the particle surface for attaching tumor targeting moieties (anti-HER2, folic acid etc.) or with stealth polymers such as Polyethylene Glycol to evade capture by the macrophages of the reticuloendothelial system. The physical properties of FDSIR820 and CDSIR820 are presented and advantages/disadvantages of both formulations from the perspective of cytotoxicity in Skov-3 cells are discussed. In-vivo bio-distribution studies were done in mice to evaluate the nanoparticles for NIR imaging applications.

2. Results and Discussion

2.1 Nanoparticle Synthesis and Drug Entrapment

Doxorubicin hydrochloride (DOX-HCL) is an amphiphilic drug moiety due to a lipophilic anthraquinone part and a hydrophilic sugar ring. In order to increase the interaction between silica nanoparticles in the oil phase (Dimethylsulfoxide; DMSO) and DOX molecules, DOX-HCL was converted to its hydrophobic form (DOX) by the addition of Triethylamine (TEA). Hydrophobic DOX molecules are able to partition into the oil phase upon their addition to the emulsion. Furthermore, at high basic pH of the aqueous phase, most DOX molecules exist in neutral form^{12,13} and are therefore loaded on the silica particle surface via physical adsorption. For the conjugate, reaction between DOX and 3-(Triethoxysilyl) propyl isocyanate (ICPTES) results in a DOX-Siloxane intermediate through the formation of

urethane (-NHCOO-) or urea (-NHCONH-) linkages. However, a urea linkage could preferentially be formed due to the higher affinity of the isocyanate groups (-N=C=O) of ICPTES to the amine groups (-NH₂) of DOX.¹⁴ When DOX conjugate is added to the emulsion, the siloxane groups are hydrolyzed and DOX is covalently loaded on silica nanoparticle by condensation of siloxane groups of the conjugate with silanol (Si-OH) groups on the silica nanoparticle surface.

The FTIR-ATR spectra of Si and CDSIR820 (Figure 1) show strong absorption around 1100 cm⁻¹ due to Si-O-Si bridges commonly found in Ormosil particles. The dual split peaks in this region are red-shifted by 20–40 nm to those found in VTES sol gels. This indicates a possible porous structure.^{15,16} Sharp peaks at 1407 cm⁻¹ and 1605 cm⁻¹ indicate in plane CH₂ bending and C=C vibrations from the vinyl groups. Furthermore, the peaks at 2969 cm⁻¹ (aliphatic H-C), 3074 cm⁻¹ (aromatic H-C) and at 3400 cm⁻¹ (N-H, O-H) are due to the functional groups on the surface. The absence of peaks associated with Free DOX or Free IR820 in CDSIR820 samples is because of the additional shell growth on surface.

IR820 is physically doped and held in the silica matrix due to strong non-covalent interactions.¹⁷ The pore size of Ormosil silica nanoparticles is between 1.3–1.7 nm depending on the size of nanoparticles.¹⁸ The size of IR820 molecule, based on its molecular weight, is between 1 – 1.3 nm. Since, IR820 is doped at such a high concentration it is possible that IR820 may exist as aggregate molecules which increases their effective size and prevents leakage from the nanoparticles.

2.2 Nanoparticle Size Characterization

Ormosil/silica nanoparticles are formed through a series of steps that involve hydrolysis of the silica precursor followed by condensation and growth of particle nuclei due to intermicellar collisions. A schematic of particle preparation is shown in Figure 2. The effects of reaction parameters viz, surfactant (Dioctyl sulfosuccinate sodium salt; AOT), VTES and ammonia/3- Aminopropyltriethoxysilane (APTES) concentrations on particle size have been well studied in the literature.^{19,20} The hydrodynamic diameter of three Ormosil formulations is shown in table 1: diameter of Si was 48.5±2.5 nm, of CDSIR820 was 52.5±3.0 nm and FDSIR820 was 52.5±5.0 nm. The increase in size and polydispersity predicted by dynamic light scattering (DLS) on drug loading can be attributed to the presence of large size fraction particles as shown by the intensity distribution curve (Figure S1). It might be possible that drug loading modifies the particle surface and causes minor aggregation of particles in phosphate buffered saline. The size of our nanoparticles is ideal for passive accumulation near the tumor site due to tumor EPR.

The SEM image shows spherical particles of uniform size (Figure 3). An agreement between SEM size and average diameter predicted by DLS indicates that the hydrodynamic particle diameter in aqueous media is not increased due to particle swelling and/or aggregation. No aggregation (large aggregates, turbidity) was observed over a period of 6 hours for particles resuspended in PBS or McCoy's 5A media. Stability against aggregation in physiological buffers/solutions is a desired characteristic for designing nanoparticles for in-vivo applications. Albanese *et al.* have shown that aggregation results in a lower uptake of nanoparticles by A549 cells.²¹ Also, swelling or aggregation increases the effective

nanoparticle diameter which causes a decrease in the diffusion coefficient (diffusion coefficient is inversely related to size) and thereby limits nanoparticle penetration into tumor tissues. The size of our nanoparticles is in the ideal range for optimal cell uptake and deeper penetration into tumor. As cellular uptake of organic/inorganic nanoparticles is an energy dependent mechanism, nanoparticles with diameter less than 30 nm do not meet the energy threshold needed to drive membrane invagination and wrapping, whereas, for particles with diameter greater than 70 nm the membrane wrapping is slower and more energy intensive.²² Furthermore, nanoparticles with size more than 100 nm face significant resistance to penetration into tumor tissue due to the presence of tumor extracellular matrix and elevated intratumoral pressure which impedes nutrient and particle diffusion²³.

2.3 Absorption and Fluorescence Characteristics

The absorption curves in the supplementary figure (Figure S2) show a strong absorption in the NIR region due to IR820 and in the visible region due to DOX. The fluorescence signal of DOX in phosphate buffered saline was quenched for FDSIR820 and CDSIR820 (Figure 4). When the particles were incubated with McCoy's 5A media, the fluorescence from FDSIR820 particles increased and reached the expected free DOX value (Figure 4), whereas the signal from CDSIR820 still remained quenched. Since, DOX is in its hydrophobic form it cannot partition into aqueous media (DPBS) and the close proximity to metal surface resulted in the quenching of fluorescence signal. However, when FDSIR820 particles were re-suspended in cell culture media, DOX was able to partition into the hydrophobic components of the media or associated with serum proteins. This caused an increase in the fluorescence intensity. A similar effect on the fluorescence quenching of DOX was observed by You *et al.* when DOX was adsorbed onto a hollow gold matrix. The fluorescence subsequently increased on release of DOX from the gold matrix.²⁴

2.4 Zeta Potential

Amine grafted Ormosil particles had a zeta potential of -40.1 ± 2.3 mV in phosphate buffered saline (pH 7.4) (Table 1). There are no differences between the zeta potentials of bare Si and drug loaded formulations owing to the growth of a silica shell over the drug layer. In the case of the Ormosil particles, the zeta potential is not determined by the surface groups such as amine (from APTES functionalization) and vinyl (from VTES monomer), instead, it is determined by the type of surfactant moieties (i.e. Brij-40, Tween-20, AOT etc.) that are immobilized in the silica matrix. Severstel *et al.* reported that Ormosil nanoparticles prepared with surfactant Brij40 retained the surfactant in silica matrix despite several rigorous washing processes.²⁵ Their particles had a zeta potential of -9.3 mV. The zeta potential shifted to positive side on incubation with McCoy's 5A medium containing 10% FBS (Table 1). This is due to the adsorption of serum proteins onto the nanoparticle surface.²⁶ Adsorption of serum proteins happens very rapidly (0.5 minutes) and results in formation of a protein corona around the silica nanoparticle. The protein corona is comprised mainly of proteins with molecular mass >60 kDa. Proteins with negative charge seem to preferentially adsorb onto silica nanoparticle surfaces irrespective of the surface zeta potential (i.e. positive or negative). This results in an overall negative charge for Ormosil particles in the presence of serum.^{26,27} The protein corona on silica nanoparticles is highly enriched with apolipoproteins involved in lipid and cholesterol transport.²⁷ Formation of

protein corona on nanoparticle surface has been shown to be one of the most fundamentally important phenomena in determining nanoparticle interaction with cells.²⁸

2.5 Drug and Dye Retention

Figure 5 shows that DOX and IR820 are slowly released from FDSIR820 and CDSIR820 particles. At 48 hours approximately $93.2\% \pm 1.5\%$ Dox was retained in CDSIR820 formulation and $77.0\% \pm 1.0\%$ DOX was retained by FDSIR820 formulation. The slow release of DOX from FDSIR820 is due to the hydrophobic nature of DOX and that of CDSIR820 is due to the gradual hydrolysis of the urea bond in PBS. A similar release profile was observed for DOX-ICPTES conjugated magnetic particles by Li et al¹⁴, only 13.3 % DOX was released in 11 days from the particles. Exposure to laser caused the release of DOX from CDSIR820 particles in a time dependent manner. At 96 hours, approximately 57 % of DOX was released in response to single laser exposure of 3 minutes. It has to be noted that this release was in response to a single exposure to laser. CDSIR820 were able to generate heat 3 times upon 3 consecutive laser exposures of 3 minutes each. Although at this point the mechanism of release is unclear, hyperthermia and laser exposure may be playing a role in triggering DOX release. Successive exposure to laser might therefore be used to trigger DOX release in an on-demand fashion. Additionally, the release of DOX from CDSIR820 in physiological milieu may be enhanced under low pH conditions, such as those encountered in deep tumor regions and inside the cell lysosomes due to hydrolysis of the urea bond.

It is interesting to note that IR820 is retained in FDSIR820 ($86.2\% \pm 1.6\%$) and CDSIR820 ($94.0\% \pm 1.0\%$) at 48 hours despite being a hydrophilic dye. The physical confinement of IR-820 aggregate molecules in the rigid silica matrix and additional shell on surface is the reason behind slow release. This is advantageous for planning simultaneous imaging and adjuvant hyperthermia at the tumor site.

2.6 Cell Uptake

DOX is a DNA intercalating agent that prevents DNA replication by binding with the topoisomerase II complex of cell DNA. Therefore, DOX in its free form is transported to the nucleus which is evident from Figure 6 (Free DOX). Similarly, when cells are incubated with FDSIR820 for 12 hours DOX fluorescence is present in the nucleus (Figure 6). This is due to labile DOX partitioning into lipid bubbles in the cell membrane due to its hydrophobicity and thus enters the cell and binds with the nucleus in its free form. Conversely, incubation with CDSIR820 resulted in distinct fluorescent puncta in the cell cytoplasm and faint nuclear staining (Figure 6). These observations are in accordance with the results by Salvati et al. who showed that the presence of labile dye on polystyrene nanoparticles results in a diffuse fluorescence, whereas nanoparticles with a non-labile dye appear as distinct fluorescent puncta.²⁹

DOX fluorescence from CDSIR820 merges with the fluorescence from lysotracker red (Figure 6) suggesting that CDSIR820 particles eventually localize in the cell lysosomes. Also, there is a weak DOX fluorescence from the nuclear region (compared to FDSIR820) possibly due to slow urea bond hydrolysis and release of DOX from CDSIR820

nanoparticles. The cellular uptake mechanisms of Ormosil nanoparticles are not well understood. Studies by Shapero et al. have shown that cell uptake of amorphous silica nanoparticles with similar size (50 nm) and surface properties (zeta potential) is an energy dependent process in which the endocytic uptake mechanisms that are clathrin or caveolae mediated are not involved.³⁰ Fifty nanometer silica nanoparticles enter the cell one by one through membrane invaginations, are subsequently transported to early endosomes and finally get trapped irreversibly in the lysosomes. However, no evidence of clathrin or caveolae was obtained by the authors through short term immunostaining with respective antibodies.³⁰ More recent TEM evidence by Moret et al. of cells incubated with Ormosil nanoparticles showed the presence of clathrin coated pits, however the co-localization of particles within the pits was not found.³¹ Therefore, it is possible that due to the surface protein corona, silica particles may enter the cell via more specific receptor mediated pathways that are mediated by apolipoproteins.³² Other transport mechanisms such as phagocytosis or macropinocytosis may also be involved.³³ Further studies are needed to confirm this hypothesis.

2.7 Cell Cytotoxicity

The cytotoxicity results in figure 7 show that Si and CDSIR820 nanoparticles are well tolerated by Skov-3 cells and no growth inhibition is observed below 150 µg/ml nanoparticle concentration. Meanwhile, FDSIR820 nanoparticles showed severe toxicity at relatively lower concentrations than Si and CDSIR820 formulations. Ninety four percent growth inhibition was observed in Skov-3 cells when administered 150 µg/ml FDSIR820 nanoparticles. These results are in accordance with Roy et al. who observed a significant reduction in cell viability (~80%) of MiPaCa-2 pancreatic cells treated with DOX loaded Ormosil particles.¹⁸ Furthermore, Moret et al. have shown that unpegylated blank Ormosil nanoparticles were well tolerated by NCIH-2347 adenocarcinoma and CCD-34Lu normal fibroblast cells up to a concentration of 200 µg/ml³¹. The toxicity of Ormosil nanoparticles in cancer cells is dependent on cell type and relies on disruption of various vital cell functions. Ormosil nanoparticles have been shown to induce structural changes in cell morphology, alter cell membrane permeability and metabolism, cause the generation of reactive oxygen species and promote inflammatory gene expression.³¹ Additionally, the rapid release of DOX from FDSIR820 and binding with the nucleus might explain the severe toxicity caused by this formulation. Rapid release of drug from nanoparticles is disadvantageous to in-vivo applications as it will cause systemic toxicity associated with the drug and may also reduce available injected dose of DOX to the tumor. Therefore, FDSIR820 particles were not further tested for their cell killing potential in combination with adjuvant NIR hyperthermia or *in-vivo*.

Under continual exposure to 808 nm NIR laser for 3 minutes, the temperature of media containing CDSIR820 nanoparticles reached 43°C (from 37°C) within 1 minute and stayed constant for an additional 2 minutes. The nanoparticles were able to generate heat 3 times upon 3 consecutive laser exposures of 3 minutes each. By the fourth exposure, no heat was generated owing to photo bleaching of IR820 in the particles. The ability to generate heat multiple times offers the advantage for long term adjuvant hyperthermia planning for efficient tumor eradication. Photobleaching of IR820 on NIR laser exposure can be

considered a disadvantage compared to gold nanoparticles. However, the physiological stability and small size make Ormosil particles a potential candidate for NIR imaging. Gold nanoparticles for NIR imaging and hyperthermia are usually in the size range of 150–200 nm and aggregate in physiological solutions without surface modification (i.e. PEGylation).

Laser exposure of Blank Si particles did not elicit any cytotoxic response in Skov-3 cells. SIR820 particles (loaded only with IR820) caused comparable toxicity as free DOX. This is due to rapid temperature raise which delivers greater thermal dose compared to slow rate hyperthermia and has been shown to be cytotoxic to Skov-3 cells. The combination of NIR hyperthermia and CDSIR820 (single laser exposure) resulted in significantly greater reduction in cell viability compared to Free DOX treatment (Figure 7). This is explained based on the chemotherapeutic insensitivity of Skov-3 cells due to a p53 gene deletion.³⁴ In our previous studies we have shown that an increased intracellular accumulation of DOX in Skov-3 cells by anti-HER-2 labeled PLGA particles did not translate to higher cell growth inhibition/ killing compared to Free DOX.³⁵ However, the addition of hyperthermia as an adjuvant resulted in enhanced cytotoxicity in the Skov-3 cells.³⁶ Moreover, hyperthermia can be beneficial for inhibiting p53 deficient tumor cells as it has been shown that the cellular response to hyperthermia is independent of p53 status. In a study by Fukami et al. hyperthermia led to an apoptosis-inducing factor translocation and apoptotic cell death in p53-mutant human glioma cells.³⁷

2.8 Bio-distribution Studies

The fluorescence intensity of animal organs was measured following intravenous administration of CDSIR820 particles using an NIR imaging system operating at 800 nm wavelength. Infrared (Near/Far) wavelengths are beneficial for in-vivo therapy/diagnosis as the attenuation and scattering of laser light by surrounding tissues is minimal. Strong IR820 fluorescence signal was obtained from the excised organs (figure S2). From the calculated injected dose it is clear that a major fraction of the injected dose of the nanoparticles accumulate in the organs of the reticuloendothelial system (RES), including liver, lungs, kidneys and spleen. In the first 24 hours, the injected dose peaks at 30 minutes in liver and kidneys. There are two modes of sequestration of nanoparticles in the RES organs, 1) passive accumulation and 2) capture by the macrophages residing in these organs. The sinusoidal wall of the liver has discontinuous gaps in its endothelium which might result in passive accumulation of nanoparticles. The accumulation in spleen increases remarkably at 24 hours, possibly due to increased capture of nanoparticles by the macrophage cells present in the organ. This is often the case with positively or negatively charged particles whose surface is not modified with ligands such as PEG for evading the RES system.³⁸

The kinetic distribution profile in the kidneys up to 24 hours may suggest some clearance via urine, however, the size of the nanoparticles is above the threshold for glomerular filtration and subsequent excretion via kidneys. Only particulates in the size range 7–10 nm are efficiently excreted via the kidneys.³⁹ For particles above 30 nm diameter, excretion in feces via hepatobiliary clearance is a more prominent mode of removal. Since we do not expect our Ormosil particles to degrade rapidly they are more likely to be cleared via the hepatobiliary route.

The presence of particles in heart is somewhat surprising, this may be possible since silica nanoparticles have been shown to associate with vascular cells.⁴⁰ This may explain the variation observed in heart tissue, which might have been caused due to the presence of residual blood clotted in the organ. Vascular association of nanoparticles may also explain accumulation in lungs. Mesoporous and non-amine silica particles have been shown to accumulate in the lungs due to association with lung vascular cells instead of internalization by pulmonary cells.⁴⁰ Furthermore, the particle surface may be gradually modified due to the hydrolysis of amide bonds which happens in-vivo (in liver).⁴¹ A bright fluorescence signal from lungs was observed at 6 hours (CDSIR820) and was still present at 48 hours in the animals administered with free IR820 and CDSIR820 (Figure S3). Ravi et al confirmed that encapsulated dye can redirect the nanoparticles to its primary site of accumulation. Another reason for lung accumulation might be due to some aggregation of our particles, as indicated by the DLS measurements. The bio distribution data (Figure S4) suggests that after 24 hours, Ormosil nanoparticles are retained more in the spleen than the free dye. Additional studies of plasma clearance are needed to get a quantitative parameters viz circulation time, plasma clearance half-life etc. of our nanoparticles. However, recent reports from Qian et al with IR820 loaded Ormosil particles showed sustained particle fluorescence at the tumor site until 30 days¹⁷.

It is important to note that even though Ormosil particles may not possess cytotoxic effects at low concentrations, vascular obstruction due to the formation of aggregates may pose a health hazard and hence strategies to further enhance particle stability and evade RES capture are needed. In a study by our group with IR820 PEG diamine particles, we found that free IR820 localized in liver and lungs after 24 hours, but IR820-PEG-diamine conjugates did not show any lung accumulation, presumably due to the presence of PEG.

3. Experimental Methods

3.1 Synthesis of DOX-ICPTES conjugate

Five milligrams DOX-HCL was reacted with 2 mole excess Triethylamine (TEA) in 500 μ l anhydrous DMSO. This solution was vigorously stirred for 6 hours at room temperature in the dark followed by the addition of 20 μ l 3-(Triethoxysilyl) propylisocyanate (ICPTES). The reaction was allowed to proceed for 18 hours and the product (DOX-ICPTES) was used without further purification.

3.2 Synthesis of IR820 and DOX loaded organically modified silica nanoparticles

Organically modified silica nanoparticles (Ormosil) were prepared by a modification of the ternary microemulsion method developed by Prasad and colleagues.⁶ Briefly, 0.44 mg of Dioctyl sulfosuccinate sodium salt (AOT) was dissolved in 20 ml of deionized water followed by the addition of 800 μ l 1-butanol resulting in a clear solution. To this, 800 μ l of DMSO containing IR820 (25 mM) was added. Void nanoparticles were created by adding DMSO without the dye. After this, 125 μ l of the silica precursor Triethoxysilane (VTES) was added and stirred for 30 minutes. Ormosil nanoparticles were precipitated by the addition of 20 μ l aqueous ammonium hydroxide (NH₄OH; 28 % in water) and stirring for 18 hours at room temperature.

For DOX loading, 500 μ l of free DOX in DMSO or 500 μ l DOX-ICPTES in DMSO was added along with 75 μ l VTES to the precipitated particles and stirred for 6 hours. An additional shell of silica was grown by adding 100 μ l of VTES. Amine groups were grafted on the surface by the addition of 10 μ l 3- Aminopropyltriethoxysilane (APTES) 30 minutes after the addition of VTES. Finally, after 18 hours of additional stirring the obtained particles were dialyzed for 50 hours using a 12–14 kDa cellulose membrane to remove the free dyes/drugs (IR820, DOX), the surfactant AOT and the co-surfactant 1-butanol. The dialyzed particles were refrigerated until further use. Blank Ormosil nanoparticles without any dye and drug are referred to as Si, with unconjugated DOX are referred to as FDSIR820 and nanoparticles with DOX-ICPTES conjugate are denoted as CDSIR820. The size and zeta-potential of Ormosil formulations were characterized using Dynamic Light Scattering (DLS) and Scanning electron microscopy (SEM) (Supplementary method S1). Particle composition was studied using FTIR-ATR (Supplementary method S1) and absorption/fluorescence spectra were obtained using spectrofluorometer (Supplementary method S2)

3.3 Cell cytotoxicity measurement

Ovarian carcinoma cells (Skov-3) were maintained in a humidified incubator at 37 °C and 5 % CO₂. The cells were fed regularly with McCoy's 5A media supplemented with 10 % Fetal Bovine Serum (FBS) and 1% penicillin-streptomycin. For treatment, Skov-3 cells were plated in 96 well plates at a density of 5000 cells per well (200 μ l) and allowed to attach for 24 hours. Free DOX-HCL, nanoparticles Si, FDSIR820 and CDSIR820 were added at different concentrations to the cells and were incubated for 48 hours. Cytotoxicity was determined by the Sulforhodamine Blue assay (SRB).

Furthermore, Skov-3 cells were exposed to 808 nm wavelength NIR laser (1W) in the presence of nanoparticles. The cells were incubated with nanoparticles for 3 hours and were placed on a heated insert equipped to a movable stage to maintain the cells at 37 °C. The stage was moved so that each well to be exposed was directly in-line with the laser probe. The exposure time for each well was 3 minutes, which was based on our previous studies.⁵ Temperature of the well was monitored during laser exposure by a wire-thermocouple. After laser exposure, the plates were incubated for 48 hours and cytotoxicity was determined using the SRB assay. Three experiments with 3 replicates each were performed.

3.4 Imaging of nanoparticle uptake

Skov-3 cells were grown on poly-L-lysine coated coverslips and transfected with Cell BacMam lysolight RFP[®]. Then, they were incubated with free DOX and DOX loaded nanoparticles (FDSIR820, CDSIR820) for twelve hours, stained with 4',6-diamidino-2-phenylindole (DAPI), washed 3 times with ice cold DPBS, fixed with 4 % formalin and mounted onto a glass slide. Images were acquired using a Deltavision[®] deconvolution microscope at the respective wavelengths of the dyes i.e. DAPI (λ_{ex} : 360 nm, λ_{em} : 430 nm), DOX (λ_{ex} : 480 nm, λ_{em} : 590 nm) and lyso-RFP (λ_{ex} : 550 nm, λ_{em} : 610 nm). It should be noted that imaging at DOX wavelengths is only to illustrate the subcellular localization of Ormosil particles, the goal of *in-vivo* imaging in NIR region is achieved by IR820 as explained below.

3.5 Bio-distribution of Ormosil nanoparticles

ICR mice were in-bred and kept under standard housing conditions, and fed ad libitum. All protocols followed the regulations of the Institutional Animal Care and Use Committee. Mice were randomly assigned to different experimental groups based on different time points, namely 15 minutes, 30 minutes, 60 minutes, 6 Hours, 24 hours and 48 hours. On the day of the experiment, the animals were anesthetized with isoflurane and injected i.v. through the tail vein with a solution of NPs in PBS. The concentration of injected NPs was determined based on an IR820 dose of 0.24 mg/kg of body weight and an injection volume of 0.1 mL (1 mg/ml Ormosil concentration). At the terminal time point for all groups (15 min, 30 min, 60 min, 24 h and 48h), the animals were euthanized and their organs were harvested. Blood samples were collected via a heart-stick.

IR820 fluorescence from the organs and blood was measured in a Li-Cor® Odyssey imaging system. Region of interests were generated for each organ and the fluorescence intensity was determined in Image J 1.39®. Fluorescence intensity of each organ was converted to particle concentration from a calibration curve obtained by mixing CDSIR820 particles with mouse blood. The particle concentration was normalized with respect to organ weight in grams.

4. Conclusion

We report the creation of novel theranostic system using Ormosil nanoparticles loaded with DOX and IR820 for chemotherapy, adjuvant hyperthermia and NIR imaging. The nanoparticles have physical characteristics viz size and aqueous stability optimal for cell uptake and deep penetration into tumors. Covalent loading of DOX on the silica particle surface slowed the release of DOX compared to physical adsorption, which resulted in rapid release of DOX from the particles. Exposure to near infrared laser caused an increase in temperature and also resulted in release of DOX. The comparison of cytotoxicity profiles between different loading modes show that FDSIR820 causes high toxicity in Skov-3 ovarian cancer cells whereas CDSIR820 particles are well tolerated by the cells. Additionally, exposure to NIR laser caused an increase in temperature and caused enhanced cell killing. CDSIR820 were able to generate high fluorescence for in-vivo imaging. CDSIR820 particles are captured by RES organs and may associate with vascular cells. The aforementioned properties show that our multifunctional Ormosil NPs may serve as useful theranostic probes for image guided chemotherapy with adjuvant hyperthermia. Future studies will aim to study the effect of multiple laser exposures on triggering drug release, the mechanism of release, cell killing and uptake mechanism in detail. Although these particles can be passively targeted to tumor site via the EPR their surface can be modified with tumor targeting moieties (HER-2, Folic acid, etc) and stealth polymers such as PEG to avoid RES capture for in-vivo theranostics.

Supplementary Material

Refer to Web version on PubMed Central for supplementary material.

Acknowledgments

The authors acknowledge the efforts of Ms. Jayleen Messina and Mr. Matthew Chacko in conducting bio-distribution studies. We also thank the Chambers Lab and Dr. Jeremy W Chambers of Herbert Wertheim College of Medicine at FIU for the use of LiCor Imaging system. Additionally, thanks to Advanced Materials and Research Institute (AMERI) at FIU for providing SEM services.

References

1. Tang Y, McGoron AJ. *Journal of Photochemistry and Photobiology B: Biology*. 2009; 97:138–144.
2. Fernandez-Fernandez A, Manchanda R, Lei T, Carvajal DA, Tang Y, Raza Kazmi SZ, McGoron AJ. *Molecular imaging*. 2012; 11:99. [PubMed: 22469238]
3. Manchanda R, Fernandez-Fernandez A, Nagesetti A, McGoron AJ. *Colloids and Surfaces B: Biointerfaces*. 2010; 75:260–267. [PubMed: 19775872]
4. Lei T, Manchanda R, Fernandez-Fernandez A, Huang Y, Wright D, McGoron AJ. *RSC advances*. 2014; 4:17959–17968. [PubMed: 24999382]
5. Tang Y, Lei T, Manchanda R, Nagesetti A, Fernandez-Fernandez A, Srinivasan S, McGoron A. *Pharm Res*. 2010; 27:2242–2253. DOI: 10.1007/s11095-010-0231-6 [PubMed: 20694526]
6. Roy I, Ohulchanskyy TY, Pudavar HE, Bergey EJ, Oseroff AR, Morgan J, Dougherty TJ, Prasad PN. *J Am Chem Soc*. 2003; 125:7860–7865. [PubMed: 12823004]
7. Kumar R, Roy I, Ohulchanskyy TY, Goswami LN, Bonoiu AC, Bergey EJ, Tramposch KM, Maitra A, Prasad PN. *Acs Nano*. 2008; 2:449–456. [PubMed: 19206569]
8. Nakamura M. *Nanotechnology Reviews*. 2012; 1:469–491.
9. Shan, L. *Molecular Imaging and Contrast Agent Database (MICAD)*. Bethesda (MD): 2004. ed. anonymous
10. Kumar P, Roy I. *RSC Advances*. 2014; 4:16181–16187.
11. Law W, Yong K, Roy I, Xu G, Ding H, Bergey EJ, Zeng H, Prasad PN. *The Journal of Physical Chemistry C*. 2008; 112:7972–7977.
12. Raghunand N, Mahoney BP, Gillies RJ. *Biochem Pharmacol*. 2003; 66:1219–1229. [PubMed: 14505801]
13. Tewes F, Munnier E, Antoon B, Okassa LN, Cohen-Jonathan S, Marchais H, Douziech-Eyrolles L, Soucé M, Dubois P, Chourpa I. *European journal of pharmaceuticals and biopharmaceutics*. 2007; 66:488–492. [PubMed: 17433641]
14. Li S, Ma Y, Yue X, Cao Z, Dai Z. *New Journal of Chemistry*. 2009; 33:2414–2418.
15. Selvestrel F, Moret F, Segat D, Woodhams JH, Fracasso G, Echevarria IMR, Baù L, Rastrelli F, Compagnin C, Reddi E. *Nanoscale*. 2013; 5:6106–6116. [PubMed: 23728482]
16. Olejniczak Z, Ł czka M, Cholewa-Kowalska K, Wojtach K, Rokita M, Mozgawa W. *J Mol Struct*. 2005; 744:465–471.
17. Qian J, Wang D, Cai F, Zhan Q, Wang Y, He S. *Biomaterials*. 2012; 33:4851–4860. [PubMed: 22484045]
18. Roy I, Kumar P, Kumar R, Ohulchanskyy TY, Yong K, Prasad PN. *RSC Advances*. 2014; 4:53498–53504.
19. Roy I, Ohulchanskyy TY, Bharali DJ, Pudavar HE, Mistretta RA, Kaur N, Prasad PN. *Proc Natl Acad Sci U S A*. 2005; 102:279–284. 0408039101 [pii]. [PubMed: 15630089]
20. Bagwe RP, Yang C, Hilliard LR, Tan W. *Langmuir*. 2004; 20:8336–8342. [PubMed: 15350111]
21. Albanese A, Chan WC. *ACS nano*. 2011; 5:5478–5489. [PubMed: 21692495]
22. Zhang S, Li J, Lykotrafitis G, Bao G, Suresh S. *Adv Mater*. 2009; 21:419–424. [PubMed: 19606281]
23. Jain RK, Stylianopoulos T. *Nature reviews clinical oncology*. 2010; 7:653–664.
24. You J, Zhang G, Li C. *ACS nano*. 2010; 4:1033–1041. [PubMed: 20121065]
25. Selvestrel F, Moret F, Segat D, Woodhams JH, Fracasso G, Echevarria IMR, Baù L, Rastrelli F, Compagnin C, Reddi E. *Nanoscale*. 2013; 5:6106–6116. [PubMed: 23728482]

26. Lesniak A, Campbell A, Monopoli MP, Lynch I, Salvati A, Dawson KA. *Biomaterials*. 2010; 31:9511–9518. [PubMed: 21059466]
27. Tenzer S, Docter D, Kuharev J, Musyanovych A, Fetz V, Hecht R, Schlenk F, Fischer D, Kiouptsi K, Reinhardt C. *Nature nanotechnology*. 2013; 8:772–781.
28. Lesniak A, Fenaroli F, Monopoli MP, Åberg C, Dawson KA, Salvati A. *ACS nano*. 2012; 6:5845–5857. [PubMed: 22721453]
29. Salvati A, Åberg C, dos Santos T, Varela J, Pinto P, Lynch I, Dawson KA. *Nanomedicine: Nanotechnology Biology and Medicine*. 2011; 7:818–826.
30. Shapero K, Fenaroli F, Lynch I, Cottell DC, Salvati A, Dawson KA. *Molecular Biosystems*. 2011; 7:371–378. [PubMed: 20877915]
31. Moret F, Selvestrel F, Lubian E, Mognato M, Celotti L, Mancin F, Reddi E. *Arch Toxicol*. 2015; 89:607–620. [PubMed: 24888373]
32. Kreuter J, Shamenkov D, Petrov V, Ramge P, Cychutek K, Koch-Brandt C, Alyautdin R. *J Drug Target*. 2002; 10:317–325. [PubMed: 12164380]
33. Vivero-Escoto JL, Slowing II, Trewyn BG, Lin VS. *Small*. 2010; 6:1952–1967. [PubMed: 20690133]
34. Bottini A, Berruti A, Bersiga A, Brizzi MP, Brunelli A, Gorzegno G, DiMarco B, Aguggini S, Bolsi G, Cirillo F, Filippini L, Betri E, Bertoli G, Alquati P, Dogliotti L. *Clin Cancer Res*. 2000; 6:2751–2758. [PubMed: 10914720]
35. Lei T, Srinivasan S, Tang Y, Manchanda R, Nagesetti A, Fernandez-Fernandez A, McGoron AJ. *Nanomedicine: Nanotechnology Biology and Medicine*. 2011; 7:324–332.
36. Srinivasan S, Manchanda R, Lei T, Nagesetti A, Fernandez-Fernandez A, McGoron AJ. *Journal of Photochemistry and Photobiology B: Biology*. 2014; 136:81–90.
37. Fukami T, Nakasu S, Baba K, Nakajima M, Matsuda M. *J Neurooncol*. 2004; 70:319–331. [PubMed: 15662973]
38. Fernandez-Fernandez, A.; Manchanda, R.; Carvajal, DA.; Lei, T.; McGoron, AJ. Covalent IR820-PEG diamine conjugates: characterization and in vivo biodistribution. *International Society for Optics and Photonics*; 2013.
39. Ernsting MJ, Murakami M, Roy A, Li S. *J Controlled Release*. 2013; 172:782–794.
40. Yu T, Hubbard D, Ray A, Ghandehari H. *J Controlled Release*. 2012; 163:46–54.
41. Kumar R, Roy I, Ohulchansky TY, Vathy LA, Bergey EJ, Sajjad M, Prasad PN. *ACS nano*. 2010; 4:699–708. [PubMed: 20088598]

Highlights

- A novel multifunctional ormosil probe for cancer theranostics.
- Physical properties of nanoparticles are optimal for passive targeting of tumors.
- Particles exhibit enhanced release of DOX in response to NIR laser exposure.
- Enhanced cancer cell killing due to combination DOX and IR820 induced hyperthermia
- Drug/Dye loaded ormosil particles show high IR820 fluorescence from RES organs.

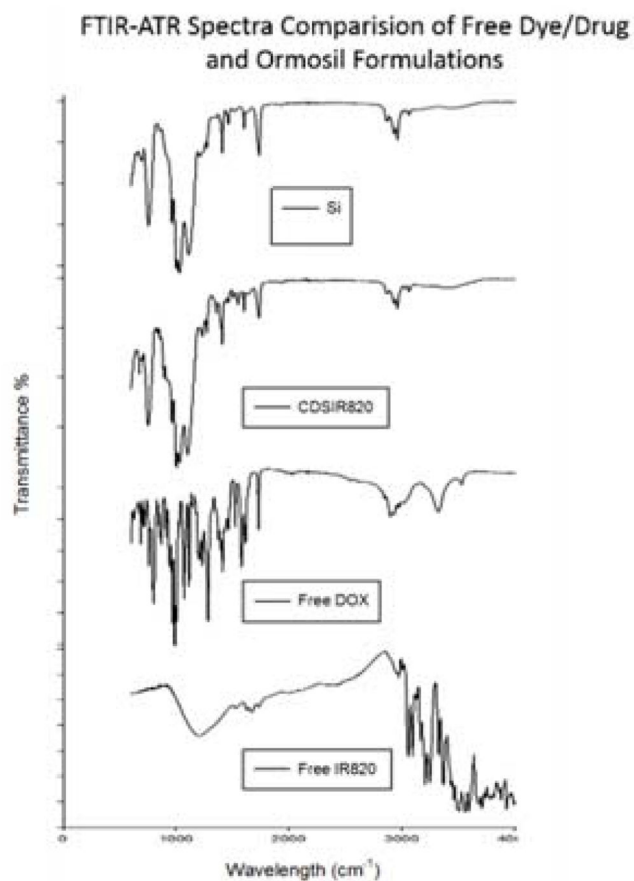


Figure 1. FTIR-ATR spectra of Blank ORM, CDSIR820, Free Dox and Free IR820. A clear overlap is seen for Blank ORM (no drug or dye) with CDSIR820 indicating the presence of additional silica shell.

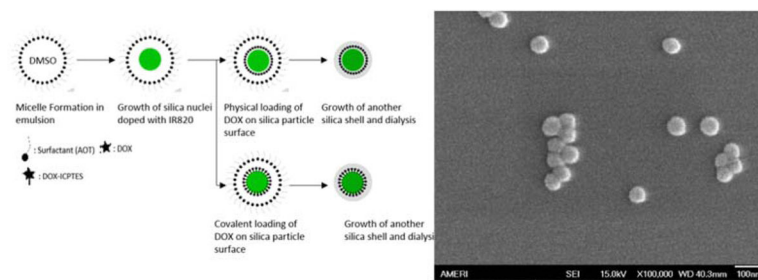


Figure 2. Schematic of nanoparticle formation in microemulsion and different modes of DOX loading (left); Scanning electron microscopy of CDSIR820 particles show monodisperse spherical particles

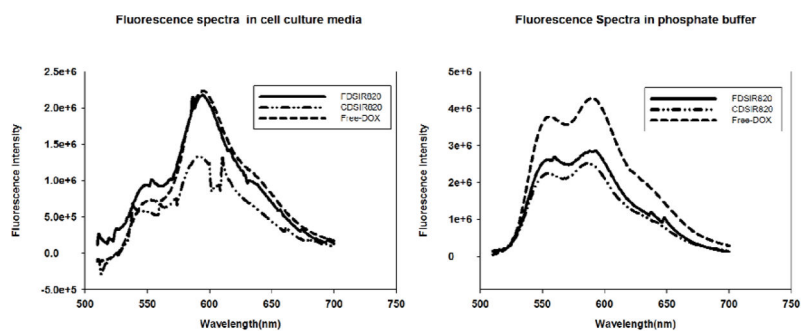


Figure 3. Fluorescence spectra of different Si formulations (3.2 μ M equivalent DOX concentration) acquired in DPBS (Right) and McCoy's 5A cell culture media (Left)

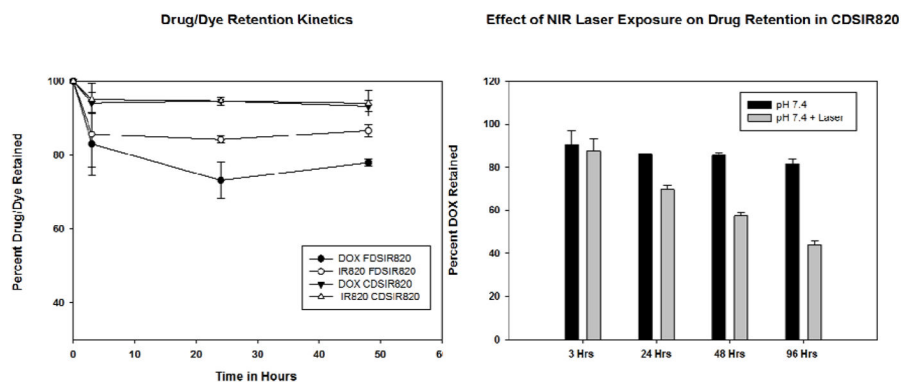


Figure 4. Retention of Drug (DOX) and Dye (IR820) in Phosphate buffered saline at 37 °C (left). CDSIR820 particles were exposed to NIR laser for 3 minutes and subsequently incubated at 37 °C for 96 hrs. Laser Exposure of CDSIR820 (right) resulted in release of DOX. IR820 release to laser exposure could not be measured accurately due to fluorescence photo bleaching of IR820. Error bars represent the standard error (SE) from 3 replicates

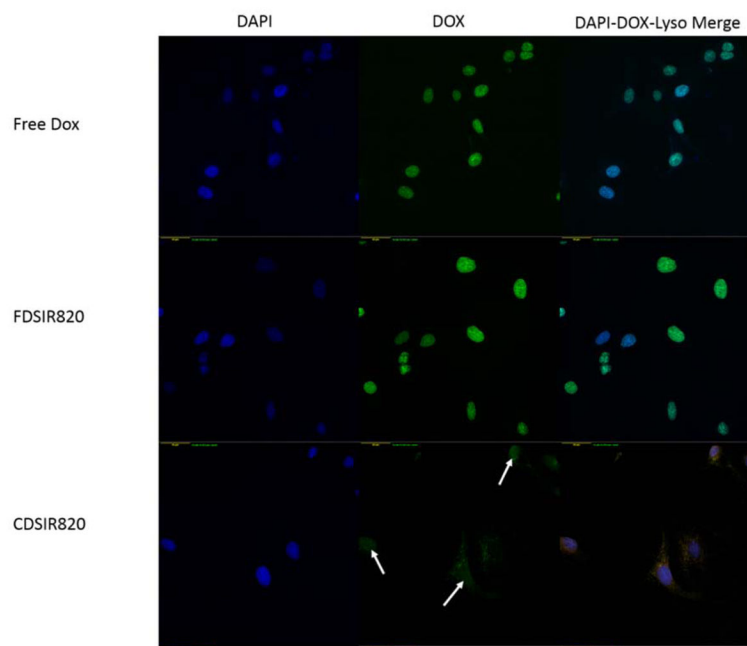


Figure 5. Fluorescence microscope images of Skov-3 cells incubated with different Ormosil formulations in different channels. Scale bar shown in left bottom corner is 40 μm . White arrows indicate DOX fluorescence from the nuclear region.

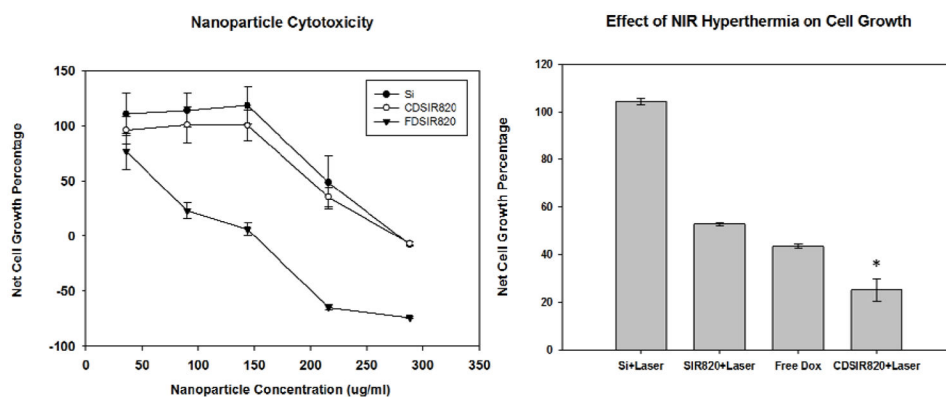


Figure 6. Cytotoxicity of different Si formulations as determined from the SRB Assay (left), effect of NIR Hyperthermia on cell killing by CDSIR820 at 100 μ g/ml (Eq DOX conc = 4.23 μ M) (right); Data is represented as mean \pm S.E for n = 3 replicates, *P < 0.05 indicates significant difference between Free Dox treatment and CDSIR820 treatment with NIR exposure.

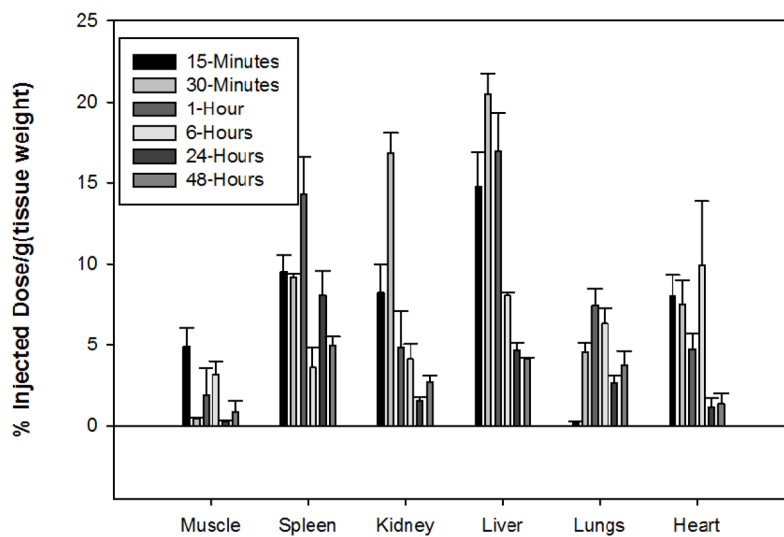
Biodistribution Profile of CDSir820 Formulation

Figure 7. Bio distribution profile of CDSIR820 up to 48 hours in different mice organs, shown as percent injected dose per gram tissue weight. Error bars represent standard error (mean \pm S.E) of 3 animals per time point.

Physical characteristics of Ormosil nanoparticles (size, distribution PDI, zeta potential in different aqueous media and drug loading). Data is represented as mean \pm S.E. for n = 6 samples

Table 1

	Diameter (nm)	PDI	Zeta Potential in DPBS (mV)	Zeta Potential in Media (mV)	IR820 Loading %(w/w)	DOX Loading %(w/w)
Si	48.5 \pm 1.0	0.061 \pm 0.015	-40.1 \pm 0.4	-14.6 \pm 0.8	N/A	N/A
FDSir8820	52.5 \pm 1.2	0.154 \pm 0.010	-39.9 \pm 0.5	-16.9 \pm 0.5	10.0 \pm 0.2	2.1 \pm 0.0
CDSir820	52.5 \pm 2.0	0.214 \pm 0.007	-41.4 \pm 0.8	-17.6 \pm 0.4	6.6 \pm 1.0	2.7 \pm 0.2